Electronic Research Archive

https://www.aimspress.com/journal/era

ERA, 32(12): 6680–6697.
DOI: 10.3934/era.2024312
Received: 27 September 2024
Revised: 25 November 2024
Accepted: 04 December 2024
Published: 12 December 2024

Research article

Dynamic optimization of a two-stage fractional system in microbial batch process

Xiaopeng Yi[1], Huey Tyng Cheong[1], Zhaohua Gong[2,3], Chongyang Liu[2,4,*] and Kok Lay Teo[1]

[1] School of Mathematical Sciences, Sunway University, Kuala Lumpur 47500, Malaysia
[2] School of Mathematics and Information Science, Shandong Technology and Business University, Yantai 264005, China
[3] School of Electrical Engineering, Computing and Mathematical Sciences, Curtin University, Perth 6845, Australia
[4] Yantai Key Laboratory of Big Data Modeling and Intelligent Computing, Yantai 264005, China

* **Correspondence:** Email: chongyangliu@aliyun.com.

Abstract: In this paper, we proposed a dynamic optimization problem involving a two-stage fractional system subjected to both a terminal state inequality constraint and continuous state inequality constraints in a microbial batch process. The objective function was the productivity of 1,3-propanediol at the terminal time, while the decision variables were the initial concentrations of biomass and glycerol, and the terminal time of the batch process. We first equivalently transformed the problem with free terminal time into one with fixed terminal time in a new time horizon by applying a proposed time-scaling transformation. We then converted the equivalent problem into an optimization problem with only box constraints by using an exact penalty function method. A novel third-order numerical scheme was presented for solving the two-stage fractional system. On this basis, we developed an improved particle swarm optimization algorithm to solve the resulting optimization problem. Finally, numerical results showed that a significant increase in the productivity of 1,3-propanediol at the terminal time was obtained compared with the previously reported results.

Keywords: two-stage fractional system; dynamic optimization; numerical scheme; particle swarm optimization; batch process

1. Introduction

1,3-Propanediol (1,3-PD) is a valuable chemical raw material widely used in various industries, including food, cosmetics, and pharmaceuticals [1]. Two commonly used methods for producing 1,3-PD are chemical synthesis and microbial fermentation [2]. Compared with chemical synthesis, microbial

fermentation offers distinct advantages, such as operational simplicity and minimal byproduct formation. These benefits have garnered increasing attention from both academia and industry. Given the impracticality of conducting numerous laboratory experiments to achieve high 1,3-PD conversion, it is essential to study dynamic optimization models for microbial fermentation.

There are three modes of glycerol bioconversion to 1,3-PD: batch culture, continuous culture, and fed-batch culture. In batch culture, the microorganism (*Klebsiella pneumoniae*) and the substrate (glycerol) are injected into the bioreactor only once at the beginning, with no further additions or removals during the culture period. In continuous culture, the substrate is continuously injected into the bioreactor at a specific rate, while the culture fluid is simultaneously removed at the same rate. In fed-batch culture, the operation alternates between batch and feeding phases. In this paper, we will focus on batch culture because of its ease of operation and high yield of 1,3-PD, while also laying a theoretical foundation for continuous and fed-batch culture processes [3]. To enhance the understanding of the microbial batch process, a nonlinear kinetic system for substrate consumption and product formation is proposed in [4]. A parameter identification problem with unknown time-delay and system parameters is introduced in [5]. Based on these mathematical models, a robust dynamic optimization problem with respect to uncertain system parameters is studied in [6]. A dynamic optimization problem with a cost sensitivity constraint is developed in [7]. A bi-objective dynamic optimization problem is discussed in [8], and a stochastic dynamic optimization problem is presented in [9]. More recently, a robust dynamic optimization problem governed by a nonlinear switched time-delay system involving an unknown time-varying function is formulated in [10]. A multi-objective dynamic optimization problem subject to a nonlinear time-delay system aimed at balancing system cost and system sensitivity is considered in [11]. Furthermore, artificial intelligence methods, such as deep learning and reinforcement learning, have been explored in various fields; see, for example, [12–14]. In [12], a multifactor prediction model incorporating a combined normalization layer and a codec is proposed to effectively address data differences and complex nonlinearity in the prediction of industrial wastewater pollutants. An antimicrobial peptide screening model based on long short-term memory neural networks with an attention mechanism is presented in [13]. In [14], multi-objective reinforcement learning is employed to obtain Pareto optimal solution sets for each objective in the control of fed-batch fermentation processes. Although the aforementioned results are of interest, they are restricted to dynamical systems with integer-order derivatives.

Fractional derivatives extend integer-order derivatives to non-integer orders, providing a powerful tool for modeling and analyzing complex systems [15]. Unlike integer-order derivatives, fractional derivatives are regarded as nonlocal operators with memory and hereditary because they take into account a broader range of historical influences. As a result, fractional dynamical systems are well-suited for representing complex phenomena characterized by memory effects. In recent years, many successful fractional models have been studied in bioengineering research. For example, in [16], fractional differential equations are used to model biological reactive systems such as tequila production, bioethanol production, and the thermal hydrolysis process, demonstrating the feasibility and effectiveness of fractional calculus in modeling biological process systems. A fractional mathematical model for erythritol and mannitol synthesis is established in [17], which proves to be useful for both prediction and process optimization. In [18], a novel cascaded control strategy based on fractional-order fuzzy proportional-derivative/proportional-integral control is proposed for temperature regulation in the fermentation process. A nonlinear fractional Michaelis-Menten enzyme kinetics model is intro-

duced in [19], and a homotopy perturbation method is developed to effectively solve this biochemical reaction process. It is worth noting that fractional modeling has also been gaining popularity in the bioconversion of glycerol to 1,3-PD. In [20], a fractional parameter identification problem is considered in the continuous culture, where the dynamical system is solved by applying the trapezoidal method and the predictor-corrector method. A single-stage fractional dynamical system with unknown kinetic parameters and fractional orders is proposed to describe the batch culture in [21]. Given that the kinetic behavior of the stationary phase described in [21] does not align well with experimental results, a new parameter identification problem involving a two-stage fractional dynamical system with different fractional orders and kinetic parameters is introduced in [22]. However, to the best of our knowledge, no study on the dynamic optimization of a two-stage fractional system in 1,3-PD batch production has been reported in the literature.

Motivated by this, in this paper, we propose a dynamic optimization problem involving the two-stage fractional system in [22] to optimize the microbial batch process, aiming to maximize the productivity of 1,3-PD at the terminal time. The decision variables of this process include the initial concentrations of biomass and glycerol, along with the terminal time of the batch process. By applying a proposed time-scaling transformation, we equivalently transform the problem with free terminal time into one with fixed terminal time in a new time horizon. By using an exact penalty function method, we convert the equivalent problem, which involves both a terminal state inequality constraint and continuous state inequality constraints, into an optimization problem with only box constraints. We then present a novel third-order numerical scheme to solve the two-stage fractional system. An improved particle swarm optimization IPSO algorithm is developed to determine the optimal decision variables. Numerical results demonstrate that the productivity of 1,3-PD at the terminal time is higher than the previous results, verifying the effectiveness of the proposed optimization strategy.

The rest of the paper is structured as follows. A two-stage fractional system is presented in Section 2. In Section 3, a dynamic optimization problem is proposed. Section 4 develops a third-order numerical scheme and an IPSO algorithm. In Section 5, numerical results are provided. Finally, concluding remarks are given in Section 6.

2. Two-stage fractional system in microbial batch process

Based on the work presented in [22], mass balance equations between biomass, substrate, and products in the microbial batch process can be modeled by the following two-stage fractional system:

$$\begin{cases} {}_0^C D_t^{\alpha^1} \boldsymbol{x}(t) = \boldsymbol{f}^1(\boldsymbol{x}(t)), & t \in (0, t_1], \\ \boldsymbol{x}(0) = \boldsymbol{x}^0, \end{cases} \tag{1}$$

$$\begin{cases} {}_{t_1}^C D_t^{\alpha^2} \boldsymbol{x}(t) = \boldsymbol{f}^2(\boldsymbol{x}(t)), & t \in (t_1, t_f], \\ \boldsymbol{x}(t_1^+) = \boldsymbol{x}(t_1), \end{cases} \tag{2}$$

where $\boldsymbol{\alpha}^1 = (\alpha_1^1, \alpha_2^1, \ldots, \alpha_5^1)^\top \in (0, 1]^5$ and $\boldsymbol{\alpha}^2 = (\alpha_1^2, \alpha_2^2, \ldots, \alpha_5^2)^\top \in (0, 1]^5$ are given vectors of fractional orders; t is the process time (in hours); $\boldsymbol{x}(t) = (x_1(t), x_2(t), \ldots, x_5(t))^\top \in \mathbb{R}^5$ is the state vector representing the concentrations of biomass, glycerol, 1,3-PD, ethanol, and acetate, respectively, with $x_1(t)$ measured in gL^{-1} and $x_i(t), i = 2, 3, 4, 5$, measured in mmolL^{-1}; t_1 is a given switching time; t_f is a free terminal time; $\boldsymbol{x}^0 \in \mathbb{R}^5$ is the initial state vector; $\boldsymbol{x}(t_1^+)$ denotes the righthand limit of $\boldsymbol{x}(t_1)$;

${}_0^C D_t^{\boldsymbol{\alpha}^1} \boldsymbol{x}(t) = \left({}_0^C D_t^{\alpha_1^1} x_1(t), \ldots, {}_0^C D_t^{\alpha_5^1} x_5(t)\right)^\top$ and ${}_{t_1}^C D_t^{\boldsymbol{\alpha}^2} \boldsymbol{x}(t) = \left({}_{t_1}^C D_t^{\alpha_1^2} x_1(t), \ldots, {}_{t_1}^C D_t^{\alpha_5^2} x_5(t)\right)^\top$ with ${}_0^C D_t^{\alpha_i^1} x_i(t)$ and ${}_{t_1}^C D_t^{\alpha_i^2} x_i(t), i = 1, 2, \ldots, 5$, denoting the α_i^1th and α_i^2th Caputo fractional derivatives of $x_i(t)$ defined by

$$ {}_0^C D_t^{\alpha_i^1} x_i(t) = \frac{1}{\Gamma(1-\alpha_i^1)} \int_0^t (t-\tau)^{-\alpha_i^1} \dot{x}_i(\tau) d\tau, \quad t \in (0, t_1], \tag{3} $$

$$ {}_{t_1}^C D_t^{\alpha_i^2} x_i(t) = \frac{1}{\Gamma(1-\alpha_i^2)} \int_{t_1}^t (t-\tau)^{-\alpha_i^2} \dot{x}_i(\tau) d\tau, \quad t \in (t_1, t_f], \tag{4} $$

with $\Gamma(\cdot)$ representing the Gamma function and $\dot{x}_i(\tau)$ denoting the first-order derivative of $x_i(\tau)$; and $\boldsymbol{f}^1 : \mathbb{R}^5 \to \mathbb{R}^5$ and $\boldsymbol{f}^2 : \mathbb{R}^5 \to \mathbb{R}^5$ describe a two-stage dynamical system in the microbial batch process, as detailed below:

$$ \boldsymbol{f}^1(\boldsymbol{x}(t)) = \begin{pmatrix} c_1 x_1(t) x_2(t) - d_1 x_1(t) \\ -c_2 x_1(t) x_2(t) + d_2 x_1(t) \\ c_3 x_1(t) x_2(t) - d_3 x_1(t) \\ c_4 x_1(t) x_2(t) - d_4 x_1(t) \\ c_5 x_1(t) x_2(t) - d_5 x_1(t) \end{pmatrix}, \quad t \in (0, t_1], $$

$$ \boldsymbol{f}^2(\boldsymbol{x}(t)) = \begin{pmatrix} c_6 x_1(t) x_2(t) - d_6 x_1(t) \\ -c_7 x_1(t) x_2(t) + d_7 x_1(t) \\ c_8 x_1(t) x_2(t) - d_8 x_1(t) \\ c_9 x_1(t) x_2(t) - d_9 x_1(t) \\ c_{10} x_1(t) x_2(t) - d_{10} x_1(t) \end{pmatrix}, \quad t \in (t_1, t_f]. $$

Here, c_j and c_{j+5}, $j = 1, 2, \ldots, 5$, are given kinetic parameters that represent biomass growth, glycerol consumption, and the formation of 1,3-PD, ethanol, and acetate, respectively. Similarly, d_j and d_{j+5}, $j = 1, 2, \ldots, 5$, are given kinetic parameters that represent the inhibitory effects of cell death on these same processes. Under anaerobic conditions at 37 °C and pH 7.0, the values of these fractional orders and kinetic parameters are listed in Table 1. Furthermore, Figure 1 depicts substrate consumption and product formation in the microbial batch process.

Table 1. The fractional orders and kinetic parameters of the two-stage system (1) and (2) [22].

Order	Value	Parameter	Value	Parameter	Value
α_1^1	9.7129E-01	c_1	1.5810E-03	d_1	1.7613E-01
α_2^1	8.8132E-01	c_2	1.6807E-01	d_2	1.0173E-01
α_3^1	7.3170E-01	c_3	1.0313E-01	d_3	2.0375E-01
α_4^1	6.2228E-01	c_4	3.0980E-02	d_4	3.8488E-02
α_5^1	8.6357E-01	c_5	3.8031E-02	d_5	3.1650E-01
α_1^2	9.8758E-01	c_6	1.7416E-03	d_6	8.6639E-04
α_2^2	8.6403E-01	c_7	2.0653E-01	d_7	2.0154E-01
α_3^2	6.9964E-01	c_8	1.8939E-01	d_8	1.1610E-01
α_4^2	9.9958E-01	c_9	6.2052E-02	d_9	2.2667E-03
α_5^2	9.7600E-01	c_{10}	5.2807E-02	d_{10}	8.3421E-04

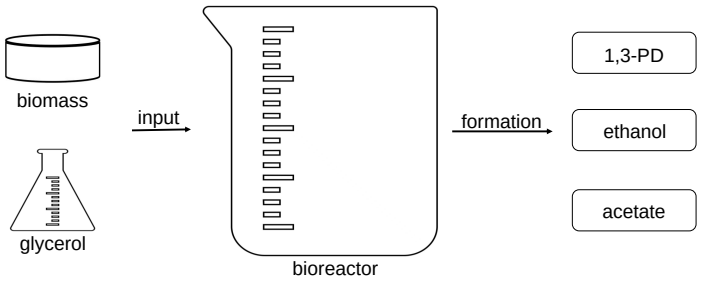

Figure 1. Substrate consumption and product formation in microbial batch process.

In the two-stage fractional system (1) and (2), the initial concentrations of the products (i.e., 1,3-PD, ethanol, and acetate) are set to $x_i^0 = 0$ for $i = 3, 4, 5$, since no products are presented at the initial time point. In contrast, the initial concentrations of biomass and glycerol are treated as decision variables to be optimized. Let $\boldsymbol{\theta} = (x_1^0, x_2^0)^\top$ and define

$$\Theta := \{\boldsymbol{\theta} \in \mathbb{R}^2 : a_m^{\min} \le \theta_m \le a_m^{\max}, m = 1, 2\},$$

where $a_m^{\min}$ and $a_m^{\max}, m = 1, 2$, are given real numbers such that $a_m^{\min} \le a_m^{\max}$. In addition, the terminal time t_f is also considered as a decision variable. Define

$$\mathcal{T} := \{t_f \in \mathbb{R} : b^{\min} \le t_f \le b^{\max}\}, \tag{5}$$

where $b^{\min}$ and $b^{\max}$ are given real numbers such that $t_1 < b^{\min} \le b^{\max}$. Any pair $(\boldsymbol{\theta}, t_f) \in \Theta \times \mathcal{T}$ is called an admissible pair for the two-stage fractional system (1) and (2).

For the two-stage fractional system (1) and (2), there exists a unique absolutely continuous solution denoted by $\boldsymbol{x}(\cdot|\boldsymbol{\theta}, t_f)$ for each $(\boldsymbol{\theta}, t_f) \in \Theta \times \mathcal{T}$ [23]. Moreover, in consideration of the practical production process, it is biologically meaningful to restrict the concentrations of biomass, glycerol, and products within the specified set W:

$$\boldsymbol{x}(t|\boldsymbol{\theta}, t_f) \in W := \prod_{i=1}^{5} [x_{*i}, x_i^*], \quad t \in [0, t_f], \tag{6}$$

where $x_{*1} = 0.01$ and $x_{*i} = 0, i = 2, 3, 4, 5$, represent the lower thresholds for the concentrations of biomass, glycerol, 1,3-PD, ethanol, and acetate, respectively, which are required for cell growth; and the corresponding upper concentration thresholds are $x_1^* = 10, x_2^* = 2039, x_3^* = 939.5, x_4^* = 360.9$, and $x_5^* = 1026$ [22].

3. Dynamic optimization problem

In the microbial batch process, glycerol is the substrate and 1,3-PD is the target product. Thus, we aim to maximize the productivity of 1,3-PD at the terminal time while minimizing the glycerol consumption rate. To achieve this, we consider the following productivity objective function:

$$\frac{x_3(t_f|\boldsymbol{\theta}, t_f)}{t_f}, \tag{7}$$

and the glycerol consumption rate constraint:

$$\frac{\theta_2 - x_2(t_f|\boldsymbol{\theta}, t_f)}{t_f} \leq \Omega, \tag{8}$$

where θ_2 denotes the initial concentration of glycerol, and $\Omega > 0$ is a predefined positive real number representing the maximum allowable glycerol consumption rate. Therefore, by combining (6)–(8), the dynamic optimization problem involving the two-stage fractional system (1) and (2) can be stated as follows:

$$\begin{aligned} \text{(P)} \qquad \min \quad & J(\boldsymbol{\theta}, t_f) = -\frac{x_3(t_f|\boldsymbol{\theta}, t_f)}{t_f} \\ \text{s.t.} \quad & \frac{\theta_2 - x_2(t_f|\boldsymbol{\theta}, t_f)}{t_f} \leq \Omega, \\ & \boldsymbol{x}(t|\boldsymbol{\theta}, t_f) \in W, \quad t \in [0, t_f], \\ & (\boldsymbol{\theta}, t_f) \in \Theta \times \mathcal{T}. \end{aligned}$$

Note that Problem (P) is a nonstandard dynamic optimization problem with two notable characteristics: (i) the terminal time t_f is free rather than fixed, and (ii) constraints (6) are continuous state inequality constraints.

To effectively handle the nonstandard characteristic (i), we will transform Problem (P), which is of a free terminal time, into an equivalent problem with a fixed terminal time in a new time horizon by employing the following time-scaling transformations. This procedure is implemented in three steps.

Step 1. $t \in [0, t_1] \to s \in [0, 1]$

Let

$$t = t(s) = t_1 s, \quad s \in [0, 1].$$

Clearly, $s = 0$ and $s = 1$ correspond to $t = 0$ and $t = t_1$, respectively. Furthermore, let $\tau = t_1\eta$ and $y_i(\eta) = x_i(t_1\eta)$. Then, we rewrite (3) as

$$\begin{aligned} {}_0^C D_t^{\alpha_i^1} x_i(t) &= \frac{1}{\Gamma(1-\alpha_i^1)} \int_0^s (t_1 s - t_1\eta)^{-\alpha_i^1} \frac{dy_i(\eta)}{d(t_1\eta)} t_1 d\eta \\ &= \frac{t_1^{-\alpha_i^1}}{\Gamma(1-\alpha_i^1)} \int_0^s (s-\eta)^{-\alpha_i^1} \dot{y}_i(\eta) d\eta = t_1^{-\alpha_i^1} {}_0^C D_s^{\alpha_i^1} y_i(s), \end{aligned}$$

for $i = 1, 2, \ldots, 5$. Let $\boldsymbol{y}(s) = \boldsymbol{x}(t_1 s)$ and ${}_0^C D_s^{\boldsymbol{\alpha}^1} \boldsymbol{y}(s) = \left({}_0^C D_s^{\alpha_1^1} y_1(s), \ldots, {}_0^C D_s^{\alpha_5^1} y_5(s)\right)^\top$. Then, fractional system (1) becomes

$$\begin{cases} {}_0^C D_s^{\boldsymbol{\alpha}^1} \boldsymbol{y}(s) = t_1^{\boldsymbol{\alpha}^1} \circ \boldsymbol{f}^1(\boldsymbol{y}(s)), \quad s \in (0, 1], \\ \boldsymbol{y}(0) = \boldsymbol{x}^0, \end{cases} \tag{9}$$

where $t_1^{\boldsymbol{\alpha}^1} = \left(t_1^{\alpha_1^1}, t_1^{\alpha_2^1}, \ldots, t_1^{\alpha_5^1}\right)^\top$; and $\circ$ represents the Hadamard product, which denotes element-wise multiplication between vectors or matrices of the same dimensions.

Step 2. $t \in (t_1, t_f] \to s \in (1, 2]$

Define

$$\Sigma := \{\sigma \in \mathbb{R} : b^{\min} - t_1 \leq \sigma \leq b^{\max} - t_1\},$$

where $b^{\min}$ and $b^{\max}$ are as defined in (5).

Let

$$t = t(s) = t_1 + \sigma(s-1), \quad s \in (1,2].$$

Clearly, $s = 2$ corresponds to $t = t_1 + \sigma = t_f$. Furthermore, let $\tau = t_1 + \sigma(\eta - 1)$ and $y_i(\eta) = x_i(t_1 + \sigma(\eta - 1))$. Then, we rewrite (4) as

$$\begin{aligned} {}_{t_1}^{C}D_t^{\alpha_i^2} x_i(t) &= \frac{1}{\Gamma(1-\alpha_i^2)} \int_1^s (\sigma s - \sigma\eta)^{-\alpha_i^2} \frac{dy_i(\eta)}{d(t_1 + \sigma(\eta-1))} \sigma d\eta \\ &= \frac{\sigma^{-\alpha_i^2}}{\Gamma(1-\alpha_i^2)} \int_1^s (s-\eta)^{-\alpha_i^2} \dot{y}_i(\eta) d\eta = \sigma^{-\alpha_i^2} {}_1^{C}D_s^{\alpha_i^2} y_i(s), \end{aligned}$$

for $i = 1, 2, \ldots, 5$. Let $\boldsymbol{y}(s) = \boldsymbol{x}(t_1 + \sigma(s-1))$ and ${}_1^{C}D_s^{\boldsymbol{\alpha}^2}\boldsymbol{y}(s) = \left({}_1^{C}D_s^{\alpha_1^2} y_1(s), \ldots, {}_1^{C}D_s^{\alpha_5^2} y_5(s)\right)^{\top}$. Then, fractional system (2) becomes

$$\begin{cases} {}_1^{C}D_s^{\boldsymbol{\alpha}^2}\boldsymbol{y}(s) = \sigma^{\boldsymbol{\alpha}^2} \circ \boldsymbol{f}^2(\boldsymbol{y}(s)), \quad s \in (1,2], \\ \boldsymbol{y}(1^+) = \boldsymbol{y}(1), \end{cases} \tag{10}$$

where $\sigma^{\boldsymbol{\alpha}^2} = \left(\sigma^{\alpha_1^2}, \sigma^{\alpha_2^2}, \ldots, \sigma^{\alpha_5^2}\right)^{\top}$.

Step 3. The restatement of Problem (P)

Let $\boldsymbol{y}(\cdot|\boldsymbol{\theta}, \sigma)$ denote the solution of the two-stage fractional system (9) and (10) for each $(\boldsymbol{\theta}, \sigma) \in \Theta \times \Sigma$. Under the time-scaling transformations (Steps 1 and 2), constraints (6) can be rewritten as

$$\boldsymbol{y}(s|\boldsymbol{\theta}, \sigma) \in W, \quad s \in [0,2], \tag{11}$$

the productivity objective function (7) is transformed into

$$\frac{y_3(2|\boldsymbol{\theta}, \sigma)}{t_1 + \sigma}, \tag{12}$$

and the glycerol consumption rate constraint (8) is reformulated as

$$\frac{\theta_2 - y_2(2|\boldsymbol{\theta}, \sigma)}{t_1 + \sigma} \le \Omega. \tag{13}$$

Therefore, Problem (P) can be restated as the following equivalent dynamic optimization problem with fixed terminal time:

$$\begin{aligned} \text{(EP)} \qquad \min \quad & \hat{J}(\boldsymbol{\theta}, \sigma) = -\frac{y_3(2|\boldsymbol{\theta}, \sigma)}{t_1 + \sigma} \\ \text{s.t.} \quad & \frac{\theta_2 - y_2(2|\boldsymbol{\theta}, \sigma)}{t_1 + \sigma} \le \Omega, \\ & \boldsymbol{y}(s|\boldsymbol{\theta}, \sigma) \in W, \quad s \in [0,2], \\ & (\boldsymbol{\theta}, \sigma) \in \Theta \times \Sigma. \end{aligned}$$

It is worth noting that Problem (EP) is a dynamic optimization problem subject to the constraints (11) and (13). Handling constraint (11) is particularly challenging numerically because it must be

satisfied at an infinite number of points over the entire time horizon. The penalty function method is a commonly used technique for handing this type of constrained optimization problems. It transforms a constrained problem into a sequence of unconstrained ones by incorporating a penalty term into the objective function. In particular, the exact penalty function method only requires a sufficiently large but finite penalty parameter to obtain a solution that satisfies the constraints and achieves the optimal objective. Therefore, to surmount the nonstandard characteristic (ii), we will employ an exact penalty function method to effectively handle these constraints.

Let

$$\begin{aligned} h_\iota(\boldsymbol{y}(s|\boldsymbol{\theta},\sigma)) &:= y_\iota(s|\boldsymbol{\theta},\sigma) - x_\iota^*, \\ h_{\iota+5}(\boldsymbol{y}(s|\boldsymbol{\theta},\sigma)) &:= x_{*\iota} - y_\iota(s|\boldsymbol{\theta},\sigma), \quad \iota = 1,2,\ldots,5. \end{aligned}$$

Then, constraint (11) is equivalent to

$$\sum_{\ell=1}^{10} \int_0^2 \max\{0, h_\ell(\boldsymbol{y}(s|\boldsymbol{\theta},\sigma))\} ds = 0. \tag{14}$$

Furthermore, we rewrite the constraint (13) as

$$\max\left\{\frac{\theta_2 - y_2(2|\boldsymbol{\theta},\sigma)}{t_1+\sigma} - \Omega, 0\right\} = 0. \tag{15}$$

Combining (14) and (15) yields the following constraint violation function:

$$\hat{H}(\boldsymbol{\theta},\sigma) := \sum_{\ell=1}^{10} \int_0^2 \max\{0, h_\ell(\boldsymbol{y}(s|\boldsymbol{\theta},\sigma))\} ds + \max\left\{\frac{\theta_2 - y_2(2|\boldsymbol{\theta},\sigma)}{t_1+\sigma} - \Omega, 0\right\}. \tag{16}$$

Obviously, $\hat{H}(\boldsymbol{\theta},\sigma) = 0$ ensures that the constraints (11) and (13) are satisfied. By incorporating $\hat{H}(\boldsymbol{\theta},\sigma)$ as a penalty term into the objective function (12), we propose the following penalty problem:

$$(\mathrm{EP}_\beta) \quad \min_{(\boldsymbol{\theta},\sigma)\in\Theta\times\Sigma} \hat{J}_\beta(\boldsymbol{\theta},\sigma) = \hat{J}(\boldsymbol{\theta},\sigma) + \beta\hat{H}(\boldsymbol{\theta},\sigma), \tag{17}$$

where $\beta > 0$ is a positive penalty parameter. Furthermore, by using a similar derivation as presented in [26], it can be proved that $\hat{J}_\beta(\boldsymbol{\theta},\sigma)$ is an exact penalty function.

4. Computational approach

In this section, we present a third-order numerical scheme for discretizing the two-stage fractional system (9) and (10). Based on this scheme, we introduce an IPSO algorithm to determine the optimal decision variables for Problem (EP_β).

4.1. Numerical scheme

For given positive integers $N^l, l = 1, 2$, we divide the intervals $(l-1, l]$ into N^l subintervals $(s_{q-1}^l, s_q^l]$ with partition points $s_q^l = (l-1) + qh^l$, where $q = 1, 2, \ldots, N^l$, and $h^l = 1/N^l$. Specifically, $s_0^1 = 0$

and $s_0^2 = 1$. Then, the two-stage fractional system (9) and (10) can be transformed into the following Volterra integral equations [15]:

$$y_i^l(s_q^l) = y_i^{l,0} + \frac{\delta_i^l}{\Gamma(\alpha_i^l)} \sum_{j=0}^{q-1} \int_{s_j^l}^{s_{j+1}^l} (s_q^l - \eta)^{\alpha_i^l - 1} f_i^l(\mathbf{y}(\eta)) d\eta, \tag{18}$$

for $i = 1, 2, \ldots, 5$, where

$$y_i^{l,0} := \begin{cases} x_i^0, & \text{if } l = 1, \\ y_i(1), & \text{if } l = 2, \end{cases}$$

$$\delta_i^l := \begin{cases} t_1^{\alpha_i^1}, & \text{if } l = 1, \\ \sigma^{\alpha_i^2}, & \text{if } l = 2. \end{cases}$$

Now, we subdivide the intervals $(s_0^l, s_1^l]$ for $l = 1, 2$, into $\aleph^l$ subintervals $(\varpi_{\kappa-1}^l, \varpi_\kappa^l]$ with partition points $\varpi_\kappa^l = s_0^l + \kappa\hbar^l, \kappa = 1, 2, \ldots, \aleph^l$, where $\aleph^l = \lceil 1/(h^l)^{\frac{1}{2}} \rceil$ with $\lceil \cdot \rceil$ representing the ceiling function, and $\hbar^l = h^l/\aleph^l$. Specifically, $\varpi_0^l = s_0^l$. For any $l = 1, 2$, and $i = 1, 2, \ldots, 5$, we approximate $f_i^l(\mathbf{y}(\eta))$ on the righthand side of (18) in $(\varpi_{\kappa-1}^l, \varpi_\kappa^l]$ for $\kappa = 1, 2, \ldots, \aleph^l$, by the following second-order Taylor expansion:

$$f_i^l(\mathbf{y}(\eta)) = \Lambda_\kappa^0 f_i^l + \Lambda_\kappa^1 f_i^l(\eta - \varpi_\kappa^l) + \Lambda_\kappa^2 f_i^l(\eta - \varpi_\kappa^l)^2, \tag{19}$$

where $\Lambda_\kappa^0 f_i^l$ and $\Lambda_\kappa^1 f_i^l$ are coefficients to be determined, and $\Lambda_\kappa^2 f_i^l$ is the remainder term. Omitting this remainder term, we can use the values of $f_i^l(\mathbf{y}(\varpi_{\kappa-1}^l))$ and $f_i^l(\mathbf{y}(\varpi_\kappa^l))$ to determine $\Lambda_\kappa^0 f_i^l$ and $\Lambda_\kappa^1 f_i^l$, yielding the following divided differences:

$$\Lambda_\kappa^0 f_i^l = f_i^l(\mathbf{y}(\varpi_\kappa^l)),$$
$$\Lambda_\kappa^1 f_i^l = \frac{f_i^l(\mathbf{y}(\varpi_\kappa^l)) - f_i^l(\mathbf{y}(\varpi_{\kappa-1}^l))}{\hbar^l}.$$

Substituting (19) into the first term of the sums of (18), we obtain

$$\frac{\delta_i^l}{\Gamma(\alpha_i^l)} \int_{s_0^l}^{s_1^l} (s_q^l - \eta)^{\alpha_i^l - 1} f_i^l(\mathbf{y}(\eta)) d\eta = \sum_{\kappa=1}^{\aleph^l} \left[-\frac{I_{\kappa 1}^{l,i,q}}{\hbar^l} f_i^l(\mathbf{y}(\varpi_{\kappa-1}^l)) + \left(I_{\kappa 0}^{l,i,q} + \frac{I_{\kappa 1}^{l,i,q}}{\hbar^l} \right) f_i^l(\mathbf{y}(\varpi_\kappa^l)) \right] + R_{i0}^{l,q}, \tag{20}$$

where

$$I_{\kappa 0}^{l,i,q} = \frac{(s_q^l - \varpi_{\kappa-1}^l)^{\alpha_i^l} - (s_q^l - \varpi_\kappa^l)^{\alpha_i^l}}{\Gamma(\alpha_i^l + 1)},$$
$$I_{\kappa 1}^{l,i,q} = \frac{-\hbar^l (s_q^l - \varpi_{\kappa-1}^l)^{\alpha_i^l}}{\Gamma(\alpha_i^l + 1)} + \frac{(s_q^l - \varpi_{\kappa-1}^l)^{\alpha_i^l + 1} - (s_q^l - \varpi_\kappa^l)^{\alpha_i^l + 1}}{\Gamma(\alpha_i^l + 2)},$$
$$R_{i0}^{l,q} = \frac{\delta_i^l}{\Gamma(\alpha_i^l)} \sum_{\kappa=1}^{\aleph^l} \int_{s_{\kappa-1}^l}^{s_\kappa^l} (s_q^l - \eta)^{\alpha_i^l - 1} \Lambda_\kappa^2 f_i^l(\eta - \varpi_\kappa^l)^2 d\eta.$$

Then, for any $l = 1, 2$, and $i = 1, 2, \ldots, 5$, we approximate $f_i^l(\mathbf{y}(\eta))$ on the righthand side of (18) in $(s_j^l, s_{j+1}^l]$ for $j = 1, 2, \ldots, q-1$, and $q = 2, 3, \ldots, N^l$, by the following third-order Taylor expansion:

$$f_i^l(\mathbf{y}(\eta)) = \Delta_{j+1}^0 f_i^l + \Delta_{j+1}^1 f_i^l(\eta - s_{j+1}^l) + \Delta_{j+1}^2 f_i^l(\eta - s_{j+1}^l)^2 + \Delta_{j+1}^3 f_i^l(\eta - s_{j+1}^l)^3, \tag{21}$$

where $\Delta^0_{j+1}f^l_i, \Delta^1_{j+1}f^l_i$, and $\Delta^2_{j+1}f^l_i$ are coefficients to be determined; and $\Delta^3_{j+1}f^l_i$ is the remainder term. Omitting this remainder term, we can use the values of $f^l_i(\boldsymbol{y}(s^l_{j-1}))$, $f^l_i(\boldsymbol{y}(s^l_j))$, and $f^l_i(\boldsymbol{y}(s^l_{j+1}))$ to determine $\Delta^0_{j+1}f^l_i, \Delta^1_{j+1}f^l_i$, and $\Delta^2_{j+1}f^l_i$, yielding the following divided differences:

$$\begin{aligned}
\Delta^0_{j+1}f^l_i &= f^l_i(\boldsymbol{y}(s^l_{j+1})),\\
\Delta^1_{j+1}f^l_i &= \frac{f^l_i(\boldsymbol{y}(s^l_{j-1}))}{2h^l} - \frac{2f^l_i(\boldsymbol{y}(s^l_j))}{h^l} + \frac{3f^l_i(\boldsymbol{y}(s^l_{j+1}))}{2h^l},\\
\Delta^2_{j+1}f^l_i &= \frac{f^l_i(\boldsymbol{y}(s^l_{j-1}))}{2(h^l)^2} - \frac{f^l_i(\boldsymbol{y}(s^l_j))}{(h^l)^2} + \frac{f^l_i(\boldsymbol{y}(s^l_{j+1}))}{2(h^l)^2}.
\end{aligned}$$

Substituting (21) into the $(j+1)$th term of the sums of (18), we obtain

$$\begin{aligned}
\frac{\delta^l_i}{\Gamma(\alpha^l_i)}\int_{s^l_j}^{s^l_{j+1}}(s^l_q-\eta)^{\alpha^l_i-1}f^l_i(\boldsymbol{y}(\eta))d\eta &= \frac{h^l\bar{I}^{l,i,q}_{j1}+\bar{I}^{l,i,q}_{j2}}{2(h^l)^2}f^l_i(\boldsymbol{y}(s^l_{j-1})) - \frac{2h^l\bar{I}^{l,i,q}_{j1}+\bar{I}^{l,i,q}_{j2}}{(h^l)^2}f^l_i(\boldsymbol{y}(s^l_j))\\
&\quad + \left[\bar{I}^{l,i,q}_{j0} + \frac{3h^l\bar{I}^{l,i,q}_{j1}+\bar{I}^{l,i,q}_{j2}}{2(h^l)^2}\right]f^l_i(\boldsymbol{y}(s^l_{j+1})) + R^{l,q}_{ij},
\end{aligned} \tag{22}$$

where

$$\begin{aligned}
\bar{I}^{l,i,q}_{j0} &= \frac{(s^l_q-s^l_j)^{\alpha^l_i} - (s^l_q-s^l_{j+1})^{\alpha^l_i}}{\Gamma(\alpha^l_i+1)},\\
\bar{I}^{l,i,q}_{j1} &= \frac{-h^l(s^l_q-s^l_j)^{\alpha^l_i}}{\Gamma(\alpha^l_i+1)} - \frac{(s^l_q-s^l_{j+1})^{\alpha^l_i+1}-(s^l_q-s^l_j)^{\alpha^l_i+1}}{\Gamma(\alpha^l_i+2)},\\
\bar{I}^{l,i,q}_{j2} &= \frac{(h^l)^2(s^l_q-s^l_j)^{\alpha^l_i}}{\Gamma(\alpha^l_i+1)} - \frac{2h^l(s^l_q-s^l_j)^{\alpha^l_i+1}}{\Gamma(\alpha^l_i+2)} - 2\frac{(s^l_q-s^l_{j+1})^{\alpha^l_i+2}-(s^l_q-s^l_j)^{\alpha^l_i+2}}{\Gamma(\alpha^l_i+3)},\\
R^{l,q}_{ij} &= \frac{\delta^l_i}{\Gamma(\alpha^l_i)}\int_{s^l_j}^{s^l_{j+1}}(s^l_q-\eta)^{\alpha^l_i-1}\Delta^3_{j+1}f^l_i(\eta-s^l_{j+1})^3d\eta.
\end{aligned}$$

Combining (18), (20), and (22), and then omitting the truncation errors from all remainder terms, we obtain the following numerical scheme:

$$\begin{aligned}
y^{l,q}_i = y^{l,0}_i + \delta^l_i\sum_{\kappa=1}^{\aleph^l}\left[-\frac{I^{l,i,q}_{\kappa 1}}{\hbar^l}f^l_i(\boldsymbol{y}^{l,\kappa-1,0}) + \left(I^{l,i,q}_{\kappa 0}+\frac{I^{l,i,q}_{\kappa 1}}{\hbar^l}\right)f^l_i(\boldsymbol{y}^{l,\kappa,0})\right] + \delta^l_i\sum_{j=1}^{q-1}\left\{\frac{h^l\bar{I}^{l,i,q}_{j1}+\bar{I}^{l,i,q}_{j2}}{2(h^l)^2}f^l_i(\boldsymbol{y}^{l,j-1})\right.\\
\left. - \frac{2h^l\bar{I}^{l,i,q}_{j1}+\bar{I}^{l,i,q}_{j2}}{(h^l)^2}f^l_i(\boldsymbol{y}^{l,j}) + \left[\bar{I}^{l,i,q}_{j0}+\frac{3h^l\bar{I}^{l,i,q}_{j1}+\bar{I}^{l,i,q}_{j2}}{2(h^l)^2}\right]f^l_i(\boldsymbol{y}^{l,j+1})\right\},
\end{aligned} \tag{23}$$

for $l = 1, 2, i = 1, 2, \ldots, 5$, and $q = 1, 2, \ldots, N^l$, where $\boldsymbol{y}^{l,\kappa,0}$ and $\boldsymbol{y}^{l,q}$ denote the approximations of $\boldsymbol{y}(\varpi^l_\kappa)$ and $\boldsymbol{y}(s^l_q)$ for each feasible l, κ, and q.

Based on (23), it is evident that the aforementioned numerical scheme is implicit and can be efficiently solved using Newton's method [24], which is a well-established technique for solving nonlinear equations. The following theorem presents the convergence rate of this numerical scheme.

Theorem 4.1. *Let $\hat{\boldsymbol{y}}^{l,q}$ be the numerical solution of* (23) *obtained using Newton's method for $l = 1, 2$, and $q = 1, 2, \ldots, N^l$. Then, there exists a positive constant $\hat{h} > 0$ such that $h < \hat{h}$, and the following inequality is satisfied:*

$$\|\boldsymbol{y}(s_q^l) - \hat{\boldsymbol{y}}^{l,q}\|_\infty \leq Ch^3,$$

where $\|\cdot\|_\infty$ denotes the infinity norm; $C > 0$ is a positive constant independent of $\boldsymbol{\alpha}^l$; and $h := \max_{l\in\{1,2\}}\{h^l\}$.

Proof. The proof is similar to those given for Theorems 3.1–3.3 in [25]. □

4.2. Optimization algorithm

Problem (EP_β) is a parameter optimization problem with only box constraints. While gradient-based optimization methods [27, 28] can be used to solve this problem, they are prone to getting trapped in local optima. Therefore, in this subsection, we will develop an IPSO algorithm to solve Problem (EP_β).

PSO, a global heuristic algorithm inspired by the social behavior of bird flocking and fish schooling during food searches, is widely regarded as one of the most successful nature-inspired optimization algorithms. Compared to other heuristic algorithms, such as the genetic algorithm, bat algorithm, ant colony optimization, and ecosystem based optimization, PSO is highly efficient and adaptable to a variety of dynamic environments. Due to its simple structure and minimal algorithmic parameters, PSO has gained widespread popularity across diverse fields such as power systems, control systems, networking, image segmentation, and more [29]. However, the standard PSO (SPSO) algorithm [30] is susceptible to falling into local optima. To enhance both its local and global search capabilities, we introduce a new strategy [31, 32] for updating particle velocity and position by adjusting algorithm parameters, including inertia weight, cognitive factor, and social factor. For the box constraints in Problem (EP_β), we also propose a new strategy to handle constraint violations. For brevity, let $\boldsymbol{\varrho} = (\theta_1, \theta_2, \sigma)^\top \in \mathbb{R}^3$ represent the decision vector of Problem (EP_β) in the IPSO algorithm. The main steps of the IPSO algorithm are given in Algorithm 1.

Algorithm 1 IPSO algorithm to solve Problem (EP_β).

Step 1. Initialize the total number of particles $\bar{N}$, the maximum number of iterations $I_{\max}$, the tolerance parameter ζ, the lower and upper bounds of the decision vector $\boldsymbol{\varrho}_{\mathrm{low}}$ and $\boldsymbol{\varrho}_{\mathrm{upp}}$, the minimum and maximum inertia weights $\omega_{\min}$ and $\omega_{\max}$, and the penalty parameter β.

Step 2. Initialize the variables:

(i) Set the iteration index $p := 1$.

(ii) Randomly generate $\bar{N}$ decision vectors within the range $[\boldsymbol{\varrho}_{\mathrm{low}}, \boldsymbol{\varrho}_{\mathrm{upp}}]$ and $\bar{N}$ particle velocities within the range $[\mathbf{0}, \mathbf{1}]$, denoted by $\boldsymbol{\varrho}^k(p-1)$ and $\boldsymbol{v}^k(p-1)$ for $k = 1, 2, \ldots, \bar{N}$.

(iii) Initialize the individual optimal position and the individual fitness value as $\boldsymbol{pbest}^k := \mathbf{0}$ and $\hat{J}_\beta(\boldsymbol{pbest}^k(p-1)) := +\infty$ for $k = 1, 2, \ldots, \bar{N}$. Also, initialize the global optimal position and the global optimal fitness value as $\boldsymbol{gbest} := \mathbf{0}$ and $\hat{J}_\beta^{\min} := +\infty$.

Step 3. For each $k = 1, 2, \ldots, \bar{N}$, perform the following operations:

(i) Solve the two-stage fractional system (9) and (10) using the numerical scheme outlined in Section 4.1. Then, calculate the objective function (17) and update $\hat{J}_\beta(\boldsymbol{pbest}^k(p))$ and $\boldsymbol{pbest}^k(p)$ by

$$\hat{J}_\beta(\boldsymbol{pbest}^k(p)) = \begin{cases} \hat{J}_\beta(\boldsymbol{\varrho}^k(p)), & \text{if } \hat{J}_\beta(\boldsymbol{\varrho}^k(p)) \le \hat{J}_\beta(\boldsymbol{\varrho}^k(p-1)), \\ \hat{J}_\beta(\boldsymbol{pbest}^k(p-1)), & \text{otherwise,} \end{cases}$$

$$\boldsymbol{pbest}^k(p) = \begin{cases} \boldsymbol{\varrho}^k(p), & \text{if } \hat{J}_\beta(\boldsymbol{\varrho}^k(p)) \le \hat{J}_\beta(\boldsymbol{\varrho}^k(p-1)), \\ \boldsymbol{pbest}^k(p-1), & \text{otherwise.} \end{cases}$$

(ii) Update $\hat{J}_\beta^{\min}$ and $\boldsymbol{gbest}$ by

$$\hat{J}_\beta^{\min} = \min_{k\in\{1,\ldots,\bar{N}\}} \{\hat{J}_\beta(\boldsymbol{pbest}^k(p))\}, \qquad \boldsymbol{gbest} = \arg\min_{k\in\{1,\ldots,\bar{N}\}} \{\hat{J}_\beta(\boldsymbol{pbest}^k(p))\}.$$

Step 4. If $p \ge I_{\max}$ or $\hat{J}_\beta^{\min} \le \zeta$, then $\boldsymbol{\varrho}_\beta^* = \boldsymbol{gbest}$ and stop. Otherwise, go to Step 5.

Step 5. Update $\boldsymbol{v}^k(p+1)$ and $\boldsymbol{\varrho}^k(p+1)$ by

$$v_\varsigma^k(p+1) = \omega(p)v_\varsigma^k(p) + c_1(p)r_\varsigma^{k,1}(pbest_\varsigma^k(p) - \varrho_\varsigma^k(p)) + c_2(p)r_\varsigma^{k,2}(gbest_\varsigma - \varrho_\varsigma^k(p)),$$

$$\varrho_\varsigma^k(p+1) = r_\varsigma^{k,3}\varrho_\varsigma^k(p) + (1 - r_\varsigma^{k,3})v_\varsigma^k(p+1),$$

for $k = 1, 2, \ldots, \bar{N}$, and $\varsigma = 1, 2, 3$, where $r_\varsigma^{k,1}$, $r_\varsigma^{k,2}$, and $r_\varsigma^{k,3}$ are random numbers within the range $[0, 1]$; and $\omega(p)$, $c_1(p)$, and $c_2(p)$ are defined as

$$\omega(p) = \omega_{\max} - (\omega_{\max} - \omega_{\min})\left(\frac{p}{I_{\max}}\right)^2,$$

$$c_1(p) = sin^2\left(\frac{\pi(I_{\max} - p)}{2I_{\max}}\right), \qquad c_2(p) = sin^2\left(\frac{\pi p}{2I_{\max}}\right).$$

Step 6. If ϱ_ς^k violates the bound constraint, then apply the following formula:

$$\varrho_\varsigma^k(p+1) = \begin{cases} 2\varrho_{\text{low},\varsigma} - \varrho_\varsigma^k(p+1), & \text{if } \varrho_\varsigma^k(p+1) < \varrho_{\text{low},\varsigma}, \\ 2\varrho_{\text{upp},\varsigma} - \varrho_\varsigma^k(p+1), & \text{if } \varrho_\varsigma^k(p+1) > \varrho_{\text{low},\varsigma}, \end{cases}$$

for $k = 1, 2, \ldots, \bar{N}$, and $\varsigma = 1, 2, 3$. Set $p := p + 1$, and go to Step 3.

5. Numerical results

In the numerical simulation, Algorithm 1 is implemented in a Matlab program to solve Problem (EP_β), with all computations performed on a personal computer equipped with a 2.80 GHz CPU and 16.0 GB of RAM. To solve Problem (EP_β), the initial decision vector, switching time, maximum al-

lowable glycerol consumption rate, and number of subintervals for systems (9) and (10) are set as $(0.2245\,\mathrm{gL}^{-1}, 509.8913\,\mathrm{mmolL}^{-1}, 2.0\,\mathrm{h})^{\top}$, $t_1 = 5.75\,\mathrm{h}$, $\Omega = 100\,\mathrm{mmolL}^{-1}\mathrm{h}^{-1}$, $N^1 = 500$, and $N^2 = 100$, respectively. In Algorithm 1, the parameters $\bar{N}$, $I_{\max}$, ξ, $\omega_{\min}$, $\omega_{\max}$, ϱ_{low}, ϱ_{upp}, and β are set as 50, 100, 10^{-4}, 0.4, 0.9, $(0.05, 200, 0.01)^{\top}$, $(1, 1700, 5)^{\top}$, and 100, respectively. It should be noted that the parameters in Algorithm 1 are empirically determined through numerous numerical experiments. By running Algorithm 1, we obtain the optimal decision vector $(0.05\,\mathrm{gL}^{-1}, 765.2177\,\mathrm{mmolL}^{-1}, 0.8576\,\mathrm{h})^{\top}$. As a result, the terminal time of the batch process is reduced to 6.6076 h, representing a 14.7406% decrease compared with the experimental data of 7.75 h in [4].

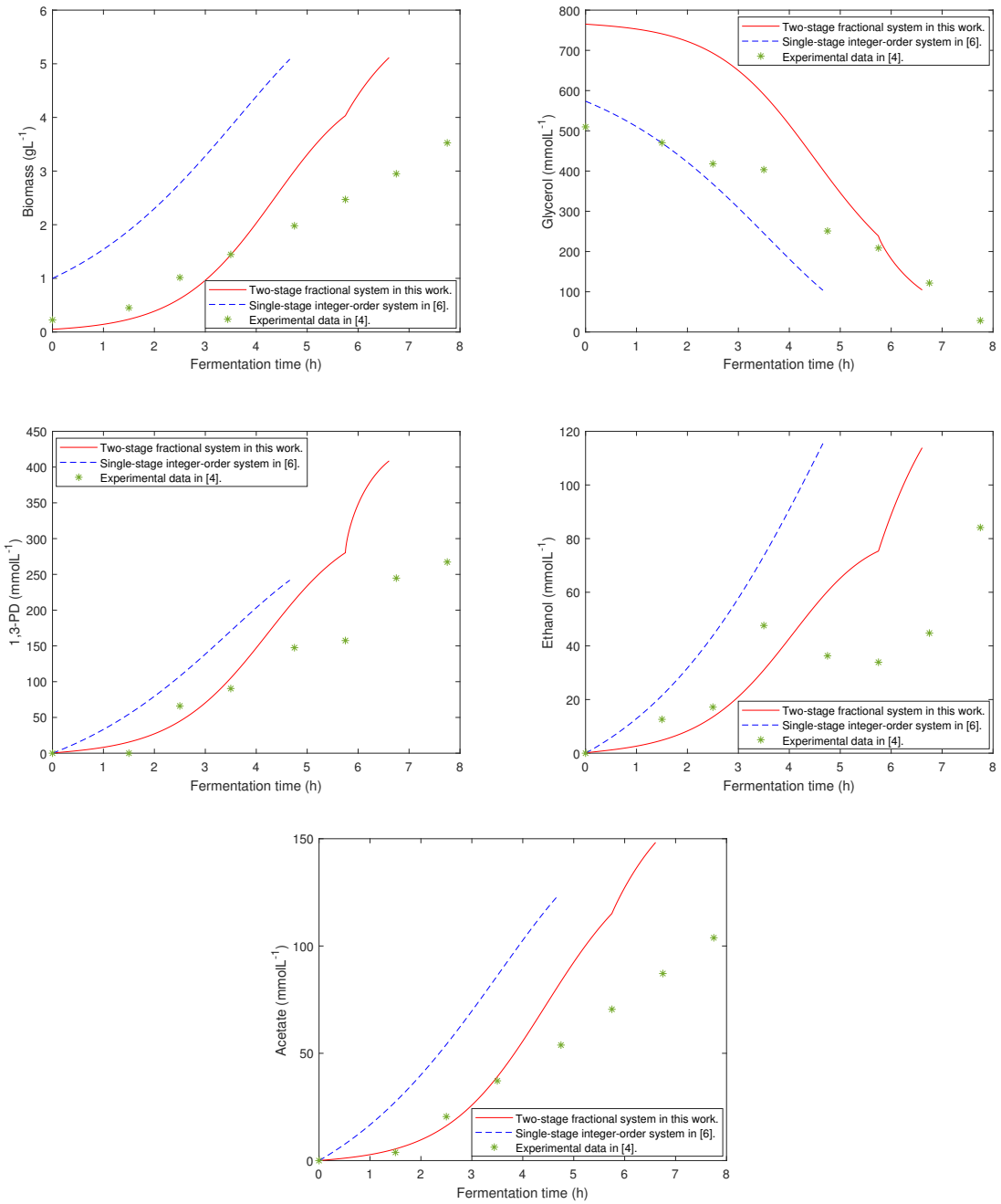

Figure 2. Changes in biomass, glycerol, and products concentrations over fermentation time.

Table 2. Computational results by using IPSO and SPSO algorithms.

Algorithm	Optimal cost	Worst cost	Average cost	Average iteration time (s)
IPSO	-61.8505	-61.8456	-61.8479	0.7702
SPSO	-61.8480	-56.6654	-61.1935	0.7666

Based on the obtained optimal decision vector, the productivity of 1,3-PD at the terminal time is determined to be 61.8505 $\text{mmolL}^{-1}\text{h}^{-1}$, showing a 79.3694% improvement compared with the 34.4822 $\text{mmolL}^{-1}\text{h}^{-1}$ observed in the experimental data from [4], and a 19.1495% improvement compared with the 51.91 $\text{mmolL}^{-1}\text{h}^{-1}$ achieved by the single-stage integer-order system in [6]. The glycerol consumption rate in our optimization model is 100 $\text{mmolL}^{-1}\text{h}^{-1}$, which is comparable to the 100.8 $\text{mmolL}^{-1}\text{h}^{-1}$ reported in [6]. Figure 2 illustrates the corresponding changes in the concentrations of biomass, glycerol, 1,3-PD, ethanol, and acetate under the optimal decision vector. Figure 3 depicts the curve of 1,3-PD productivity obtained by using the optimal decision vector. For comparison, changes in 1,3-PD productivity based on the experimental data [4] and the single-stage integer-order system [6] are also plotted in Figure 3, from which we observe that our optimization model achieves the highest productivity of 1,3-PD at the terminal time.

To further evaluate the performance of the IPSO algorithm, the SPSO algorithm is also developed to solve Problem (EP_β), with the inertia weight, cognitive factor, and social factor set to be 0.5, 2, and 2, respectively. We conduct 50 independent tests for both the IPSO and SPSO algorithms. The obtained optimal cost, worst cost, average cost, and average iteration time are listed in Table 2, from which we see that the IPSO algorithm outperforms the SPSO algorithm in terms of optimal cost, worst cost, and average cost. The average iteration time of the IPSO algorithm is comparable to that of the SPSO algorithm. The convergence curves of the objective function for both the IPSO and SPSO algorithms are depicted in Figure 4. From Figure 4, we observe that the IPSO algorithm converges significantly faster than the SPSO algorithm.

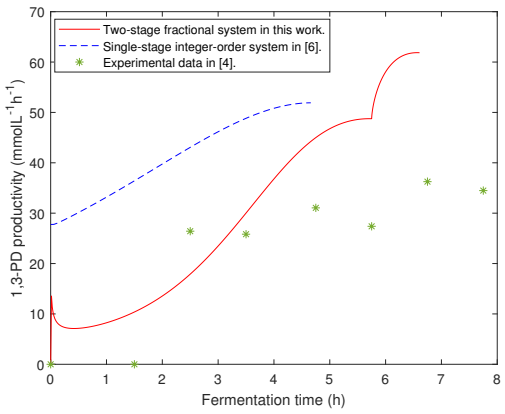

Figure 3. Changes in 1,3-PD productivity over fermentation time.

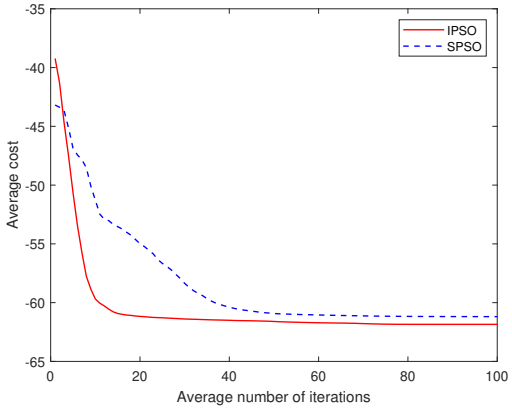

Figure 4. Convergence curves of IPSO and SPSO algorithms.

6. Conclusions

In this paper, we have proposed the dynamic optimization problem involving the two-stage fractional system subject to the terminal state inequality constraint and continuous state inequality constraints. The objective function is the productivity of 1,3-PD at the terminal time, while the decision variables are the initial concentrations of biomass and glycerol, as well as the terminal time of the batch process. The main contributions of our work include: i) the dynamic optimization problem under consideration is equivalently transformed into the one with fixed terminal time and only box constraints by applying the time-scaling transformation and the exact penalty function method; ii) we present the novel third-order numerical scheme to solve the two-stage fractional system; and iii) we develop the highly effective IPSO algorithm to determine the optimal decision variables. The numerical results show a significant increase in the productivity of 1,3-PD at the terminal time compared to previously reported outcomes, providing robust support for practical 1,3-PD batch production. In future research, we will validate the findings of this work in the real-world fermentation process. It is worth noting that, in this paper, the switching time between the two-stage fractional system is fixed. In the future, we will extend our developed method to solve the dynamic optimization of switched systems in the microbial batch process. Additionally, integrating the third-order numerical scheme with deep reinforcement learning could be a promising approach for solving large-scale fractional dynamic optimization problems.

Use of AI tools declaration

The authors declare they have not used Artificial Intelligence (AI) tools in the creation of this article.

Acknowledgments

This work is supported by the Ministry of Higher Education of Malaysia, Fundamental Research Grant Scheme (FRGS/1/2021/STG06/SYUC/03/1), the National Natural Science Foundation of China (No. 12271307), and the Natural Science Foundation of Shandong Province, China (No. ZR2023MA054).

Conflict of interest

The authors declare that they have no competing interests.

References

1. V. S. Bisaria, A. Kondo, *Bioprocessing of Renewable Resources to Commodity Bioproducts*, John Wiley & Sons Inc., New Jersey, 2014.
2. C. S. Lee, M. K. Aroua, W. M. A. W. Daud, P. Cognet, Y. Pérès-Lucchese, P. Fabre, et al., A review: Conversion of bioglycerol into 1,3-propanediol via biological and chemical method, *Renew. Sustain. Energy Rev.*, **42** (2015), 963–972. https://doi.org/10.1016/j.rser.2014.10.033
3. Y. Sun, J. Shen, L. Yan, J. Zhou, L. Jiang, Y. Chen, et al., Advances in bioconversion of glycerol to 1,3-propanediol: Prospects and challenges, *Process Biochem.*, **71** (2018), 134–146. https://doi.org/10.1016/j.procbio.2018.05.009
4. Z. Xiu, A. Zeng, L. An, Mathematical modeling of kinetics and research on multiplicity of glycerol bioconversion to 1,3-propanediol, *J. Dalian Univ. Technol.*, **40** (2000), 428–433.
5. C. Liu, Modelling and parameter identification for a nonlinear time-delay system in microbial batch fermentation, *Appl. Math. Model.*, **37** (2013), 6899–6908. https://doi.org/10.1016/j.apm.2013.02.021
6. G. Cheng, L. Wang, R. Loxton, Q. Lin, Robust optimal control of a microbial batch culture process, *J. Optim. Theory Appl.*, **167** (2015), 342–362. https://doi.org/10.1007/s10957-014-0654-z
7. J. Yuan, C. Liu, X. Zhang, J. Xie, E. Feng, H. Yin, et al., Optimal control of a batch fermentation process with nonlinear time-delay and free terminal time and cost sensitivity constraint, *J. Process Control*, **44** (2016), 41–52. https://doi.org/10.1016/j.jprocont.2016.05.001
8. C. Liu, Z. Gong, K. L. Teo, R. Loxton, E. Feng, Bi-objective dynamic optimization of a nonlinear time-delay system in microbial batch process, *Optim. Lett.*, **12** (2018), 1249–1264. https://doi.org/10.1007/s11590-016-1105-6
9. L. Wang, J. Yuan, C. Wu, X. Wang, Practical algorithm for stochastic optimal control problem about microbial fermentation in batch culture, *Optim. Lett.*, **13** (2019), 527–541. https://doi.org/10.1007/s11590-017-1220-z
10. J. Yuan, L. Wang, J. Zhai, K. L. Teo, C. Yu, M. Huang, et al., Robust optimal control for a batch nonlinear enzyme-catalytic switched time-delayed process with noisy output measurements, *Nonlinear Anal. Hybrid Syst.*, **41** (2021), 101059. https://doi.org/10.1016/j.nahs.2021.101059
11. L. Wang, J. Yuan, L. Meng, S. Zhao, J. Xie, M. Huang, et al., Multi-objective optimization of a nonlinear batch time-delay system with minimum system sensitivity, *J. Nonlinear Var. Anal.*, **6** (2022), 35–64. https://doi.org/10.23952/jnva.6.2022.2.04
12. C. Xu, J. Zhang, L. Kong, X. Jin, J. Kong, Y. Bai, et al., Prediction model of wastewater pollutant indicators based on combined normalized codec, *Mathematics*, **10** (2022), 4283. https://doi.org/10.3390/math10224283

13. Y. Liu, X. Jin, C. Xu, H. Ma, Q. Wu, H. Liu, et al., Antimicrobial peptide screening from microbial genomes in sludge based on deep learning, *Appl. Sci.*, **14** (2024), 1936. https://doi.org/10.3390/app14051936

14. D. Li, F. Zhu, X. Wang, Q. Jin, Multi-objective reinforcement learning for fed-batch fermentation process control, *J. Process Control*, **115** (2022), 89–99. https://doi.org/10.1016/j.jprocont.2022.05.003

15. I. Podlubny, *Fractional Differential Equations*, Academic Press, San Diego, 1999.

16. R. Toledo-Hernandez, V. Rico-Ramirez, G. A. Iglesias-Silva, U. M. Diwekar, A fractional calculus approach to the dynamic optimization of biological reactive systems. Part I: Fractional models for biological reactions, *Chem. Eng. Sci.*, **117** (2014), 217–228. https://doi.org/10.1016/j.ces.2014.06.034

17. E. Dulf, D. C. Vodnar, A. Danku, C. Muresan, O. Crisan, Fractional-order models for biochemical processes, *Fractal Fract.*, **4** (2020), 12. https://doi.org/10.3390/fractalfract4020012

18. V. Mohan, N. Pachauri, B. Panjwani, D. V. Kamath, A novel cascaded fractional fuzzy approach for control of fermentation process, *Bioresour. Technol.*, **357** (2022), 127337. https://doi.org/10.1016/j.biortech.2022.127377

19. B. Radhakrishnan, P. Chandru, J. J. Nieto, A study of nonlinear fractional-order biochemical reaction model and numerical simulations, *Nonlinear Anal.-Model. Control*, **29** (2024), 588–605. https://doi.org/10.15388/namc.2024.29.35109

20. D. Wang, J. Zhai, E. Feng, Fractional order modeling and parameter identification for a class of continuous fermentation, *J. Syst. Sci. Math. Sci.*, **40** (2020), 1517–1530. https://doi.org/10.12341/jssms13961

21. P. Mu, L. Wang, Y. An, Y. Ma, A novel fractional microbial batch culture process and parameter identification, *Differ. Equ. Dyn. Syst.*, **26** (2018), 265–277. https://doi.org/10.1007/s12591-017-0381-7

22. C. Liu, X. Yi, Y. Feng, Modelling and parameter identification for a two-stage fractional dynamical system in microbial batch process, *Nonlinear Anal.-Model. Control*, **27** (2022), 350–367. https://doi.org/10.15388/namc.2022.27.26234

23. K. Diethelm, *The Analysis of Fractional Differential Equations*, Springer, Berlin, 2010. https://doi.org/10.1007/978-3-642-14574-2

24. P. Deuflhard, *Newton Methods for Nonlinear Problems*, Springer, Berlin, 2011. https://doi.org/10.1007/978-3-642-23899-4

25. X. Yi, C. Liu, H. T. Cheong, K. L. Teo, S. Wang, A third-order numerical method for solving fractional ordinary differential equations, *AIMS Math.*, **9** (2024), 21125–21143. https://doi.org/10.3934/math.20241026

26. A. Xing, Z. Chen, C. Wang, Y. Yao, Exact penalty function approach to constrained optimal control problems, *Optim. Control Appl. Methods*, **10** (1989), 173–180. https://doi.org/10.1002/oca.4660100207

27. K. L. Teo, B. Li, C. Yu, V. Rehbock, *Applied and Computational Optimal Control*, Springer, Cham, 2021. https://doi.org/10.1007/978-3-030-69913-0

28. J. Yuan, D. Yang, D. Xun, K. L. Teo, C. Wu, A. Li, et al., Sparse optimal control of cyber-physical systems via PQA approach, *Pac. J. Optim.*, 2025, in Press.

29. J. Nayak, H. Swapnarekha, B. Naik, G. Dhiman, S. Vimal, 25 years of particle swarm optimization: Flourishing voyage of two decades, *Arch. Comput. Methods Eng.*, **30** (2023), 1663–1725. https://doi.org/10.1007/s11831-022-09849-x

30. J. Kennedy, R. Eberhart, Particle swarm optimization, in *Proceedings of the IEEE International Conference on Neural Networks*, (1995), 1942–1948. https://doi.org/10.1109/ICNN.1995.488968

31. C. Liu, M. Han, Time-delay optimal control problem in microbial fed-batch fermentation process, *Control Decis.*, **35** (2020), 2407–2414. https://doi.org/10.13195/j.kzyjc.2019.0254

32. C. Liu, M. Han, Time-delay optimal control of a fed-batch production involving multiple feeds, *Discrete Contin. Dyn. Syst. - Ser. S*, **13** (2020), 1697–1709. https://doi.org/10.3934/dcdss.2020099

AIMS Press